

## ORIGINAL ARTICLE

## IGFBP-2 nuclear translocation is mediated by a functional NLS sequence and is essential for its pro-tumorigenic actions in cancer cells

WJ Azar<sup>1,2</sup>, S Zivkovic<sup>1</sup>, GA Werther<sup>1,2</sup> and VC Russo<sup>1,2</sup>

IGFBP-2 is highly expressed in both the serum and tumor tissues of most cancers, and is considered one of the most significant genes in the signature of major cancers. IGFBP-2 mainly modulates IGF actions in the pericellular space; however, there is considerable evidence to suggest that IGFBP-2 may also act independently of the IGFs. These IGF-independent actions of IGFBP-2 are exerted either via interactions at the cell surface or intracellularly, via interaction with cytoplasmic or nuclear-binding partners. The precise mechanism underlying the intracellular/intranuclear localization of IGFBP-2 remains unclear. In this study, we investigated IGFBP-2 nuclear localization in several common cancer cells with the aim of dissecting the mechanism of its nuclear trafficking. IGFBP-2 is detected in the nuclei of common cancer cells, including breast, prostate and several neuroblastoma cell lines, using cell fractionation and confocal microscopy. Via nuclear import assays, we show that nuclear entry of IGFBP-2 is mediated by the classical nuclear import mechanisms, primarily through importin- $\alpha$ , as demonstrated by the use of blocking, competition and co-immunoprecipitation assays. Bioinformatics analysis of the IGFBP-2 protein sequence with PSORT II identified a classical nuclear localization signal (cNLS) sequence at <sup>179</sup>PKKLRRPP<sup>185</sup>, within the IGFBP-2 linker domain, mutagenesis of which abolishes IGFBP-2 nuclear import. Accordingly, the NLS<sub>mut</sub>IGFBP-2 fails to activate the VEGF promoter, which would otherwise occur in the presence of wild-type IGFBP-2. As a consequence, no activation of angiogenic processes were observed in NLS<sub>mut</sub>IGFBP-2 expressing SHEP cells when implanted onto our *in vivo* quail chorio-allantoic membrane model. Taken together, these data show for the first time that IGFBP-2 possesses a functional NLS sequence and that IGFBP-2 actively translocates into the nucleus by a classical nuclear import mechanism, involving formation of IGFBP-2 complexes with importin- $\alpha$ . Nuclear IGFBP-2 is required for the activation of VEGF expression and consequent angiogenesis.

Oncogene (2014) 33, 578–588; doi:10.1038/onc.2012.630; published online 25 February 2013

**Keywords:** IGFBP-2; cancer cells; VEGF; angiogenesis and CAM assay; NLS; Importin  $\alpha/\beta$

## INTRODUCTION

IGFBP-2 is the second most abundant circulating IGF-binding protein<sup>1,2</sup> and one of the most significantly expressed genes in the signature of major tumors, including prostate,<sup>3</sup> breast<sup>4,5</sup> and gliomas.<sup>6–8</sup> IGFBP-2 is recognized as a valuable prognostic biomarker for many of these cancers.<sup>3,9–13</sup> Similarly to other members of the IGFBP family, IGFBP-2 modulates IGF action in the pericellular space.<sup>1,2</sup> However, there is now increasing evidence to suggest that IGFBP-2, like other IGFBPs,<sup>1,14,15</sup> has IGF-independent actions that are exerted via cell-surface interactions<sup>1,16–19</sup> or intracellularly.<sup>20,21</sup>

We and others have shown perinuclear and nuclear localization of IGFBP-2.<sup>21–24</sup> Furthermore, we recently demonstrated that intranuclear, but not extracellular, IGFBP-2 leads to the specific activation of VEGF transcription with consequent angiogenesis *in vivo*.<sup>23</sup> The precise mechanism by which this occurs remains unknown.

In eukaryotic cells, the import of molecules into the nucleus via the nuclear pore complex is a crucial and complex event.<sup>25,26</sup> The best-characterized nuclear import pathway is mediated by a

classical nuclear localization signal sequence (cNLS; monopartite with single cluster of basic amino acids;<sup>27–29</sup> bipartite with two clusters of basic amino acids<sup>30</sup>) and the receptors importin- $\alpha$ /karyopherin- $\alpha$  and importin- $\beta$ /karyopherin- $\beta$ . In this pathway, the main determinant of nuclear localization is the presence of an NLS sequence.<sup>31–33</sup>

IGFBP-3, -5 and -6 have been shown to translocate into the nucleus<sup>1,34–37</sup> via the classical nuclear import pathway.<sup>37,38</sup> The C-terminal domains of these IGFBPs contain clusters of basic residues that resemble a bipartite cNLS, which has been shown to be required for nuclear uptake. Whether IGFBP-2 utilizes similar mechanisms for nuclear entry is yet to be determined.

The aim of this study was therefore to investigate the mechanism of IGFBP-2 nuclear import. We have extensively examined the nuclear localization of IGFBP-2 in several common cancer cells, including breast, prostate and neuroblastoma. The neuroblastoma cell line lacking endogenous IGFBP-2 (SK-N-SHEP or SHEP) was utilized to characterize the precise nuclear import mechanisms of IGFBP-2.

<sup>1</sup>Hormone Research, Murdoch Childrens Research Institute, Royal Children's Hospital, Parkville, Victoria, Australia and <sup>2</sup>Department of Paediatrics, University of Melbourne, Parkville, Victoria, Australia. Correspondence: Dr VC Russo, Hormone Research, Murdoch Childrens Research Institute, Royal Children's Hospital, Flemington Road, Parkville, Victoria 3052, Australia.

E-mail: vince.russo@mcri.edu.au

Received 4 June 2012; revised 11 November 2012; accepted 5 December 2012; published online 25 February 2013

## RESULTS

IGFBP-2 is present in the nuclei of common cancer cells MCF-7 (breast), LnCaP (prostate) and SK-N-MC, SH-SY5Y and IMR32 neuroblastoma cell lines were subjected to cell fractionation. The resultant cytoplasmic and nuclear fractions were analyzed by SDS-PAGE/immunoblotting for IGFBP-2, GAPDH as the cytoplasmic marker and Histone H3 as the nuclear marker. A specific band at 32 kDa was identified by immunoblotting as intracellular IGFBP-2, in whole cell lysates from MCF-7 and LnCaP cells (Figure 1a). A 32 kDa band was also detected in the cytoplasmic and nuclear fractions of all cancer cell lines analyzed (Figure 1b). The majority of intracellular IGFBP-2 was localized to the cytoplasm, while only a small portion was intranuclear. Owing to the nuclear fractions requiring longer film exposure, Figure 1b is only indicative of the presence or absence of IGFBP-2 in each fraction, not their relative quantities.

The subcellular localization of endogenous IGFBP-2 in MCF-7 and LnCaP cells was demonstrated by immunofluorescence, as shown in Figure 1c. Consistent with the cell fractionation data, IGFBP-2 was detected throughout the cell, and in the cytoplasm

and nuclei (merged IGFBP-2 and 4',6-diamidino-2-phenylindole staining) of both cell lines. Normal IgGs, used as the negative control, confirmed anti-IGFBP-2 antibody specificity. To confirm that intranuclear staining was due to nuclear and not cell membrane-bound IGFBP-2, three-dimensional confocal analysis of IGFBP-2 immunofluorescence was carried out (see also Supplementary Figures S1A and S1B).

IGFBP-2 is imported into the nucleus via a classic nuclear import pathway

To determine whether IGFBP-2 enters the nuclear compartment via diffusion or through an active transport mechanism, we used an *in vitro* transport assay that we have previously described for IGFBP-2.<sup>23</sup> As shown in Figure 2, digitonin-permeabilized neuroblastoma SHEP cells (which do not express any IGFBPs) were exposed to IGFBP-2 under different conditions. The subcellular localization of IGFBP-2 was detected by immunofluorescence and analyzed by laser scanning confocal microscopy. IGFBP-2 nuclear import assays were carried out in the presence of both ATP (an energy generating system) and RRL (rabbit reticulocyte lysate,

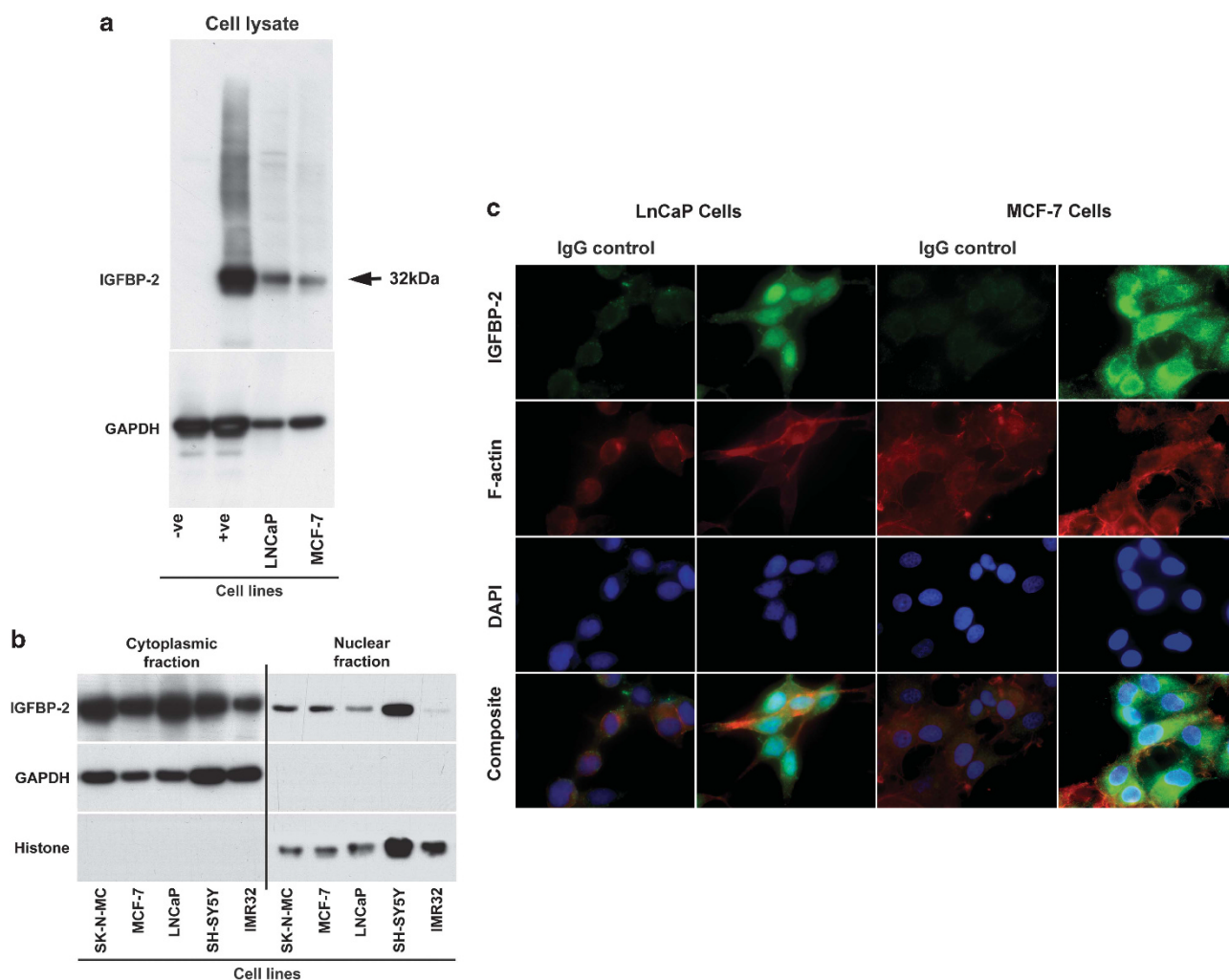


**Figure 1.** IGFBP-2 localizes in the nuclei of common cancers. (a) Western immunoblot of cell lysate from LNCaP and MCF-7 cells to confirm the presence of IGFBP-2 and specificity of the IGFBP-2 antibody. Cell lysate from SHEP-pCMV (–ve) and SHEP-WT-IGFBP-2 (+ve) cells is also included. (b) Cell fractionation of breast (MCF-7), prostate (LnCaP) and neuroblastoma (SK-N-MC, SH-SY5Y and IMR32) cancer cells demonstrated that IGFBP-2 is present in both the cytoplasmic and nuclear compartments. (Histone H3, nuclear marker; GAPDH, cytoplasmic marker). (c) Immunofluorescence showing IGFBP-2 nuclear localization in MCF-7 and LnCaP cells. Images are representative of at least three independent experiments. Cells were visualized by laser scanning confocal microscope (Leica TCS SP2 SE, objective  $\times 63$ , oil immersion).

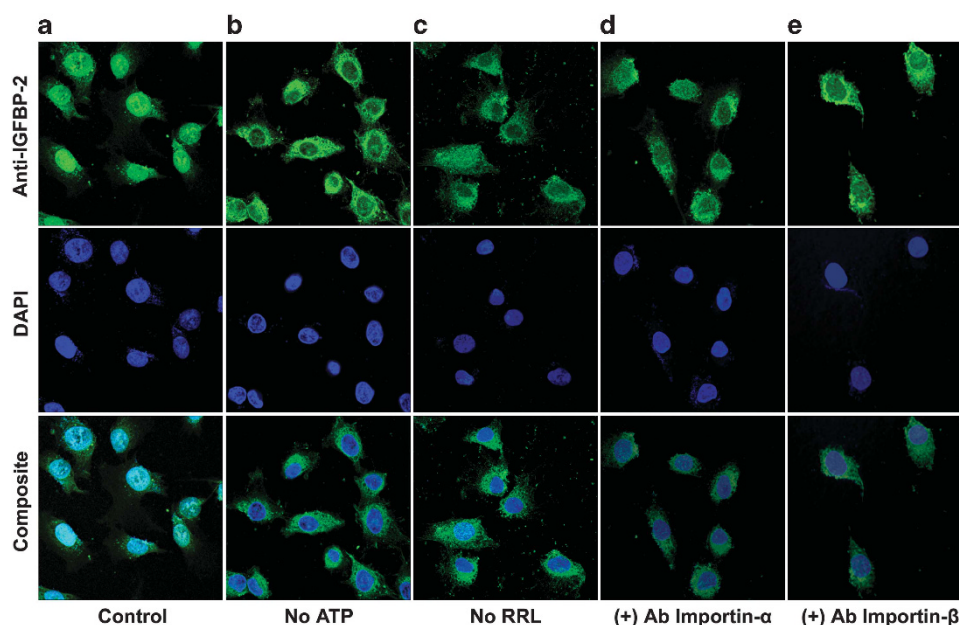


**Figure 2.** IGFBP-2 is actively transported into the nuclear compartment. IGFBP-2 nuclear localization was detected using immunofluorescence. (a) Digitonin-permeabilized SHEP cells were incubated with full-length IGFBP-2 in the presence of cytosolic factors (RRL) and an ATP-regenerating system (ATP). (b) Depletion of ATP and cytosol (c) from the import assay. Transport studies were also carried out with the addition of anti-importin- $\alpha$  (d) or - $\beta$  (e) antibodies. Images are representative of at least three independent experiments. Cells were visualized by laser scanning confocal microscope (Leica TCS SP2 SE, objective  $\times 63$ , oil immersion).

containing cytosolic factors and carriers), as shown in Figure 2a, and in the absence of ATP (Figure 2b) or RRL (Figure 2c). In comparison with the control, the absence of ATP or RRL resulted in no nuclear uptake of IGFBP-2, suggesting that nuclear import of IGFBP-2 is an energy-dependent process, and requires the presence of cytosolic factors/carriers. As nuclear import of IGFBP-3, -5 and -6<sup>37,38</sup> has been shown to require importin- $\beta$  and/or importin- $\alpha$ , we therefore utilized specific antibodies for importin- $\alpha$  and - $\beta$  to examine their role in IGFBP-2 nuclear import. To immuno-deplete importin- $\alpha$ , RRL (a source of importin- $\alpha$ ) was pre-incubated with the anti-importin- $\alpha$  antibody. To immuno-deplete importin- $\beta$ , digitonin-permeabilized cells were pre-incubated with anti-importin- $\beta$ , in the absence of RRL, before carrying out the import assay for IGFBP-2. Similar to the anti-importin- $\beta$  blocking antibody,<sup>39–41</sup> anti-importin- $\alpha$  produced an inhibitory effect on IGFBP-2 nuclear import. As shown in Figure 2d, in the presence of anti-importin- $\alpha$ , and to a lesser extent in the presence of anti-importin- $\beta$  (Figure 2e), we observed a significant reduction in nuclear accumulation of IGFBP-2. These data indicate that importin- $\alpha$  and, by inference, the importin- $\alpha$ - $\beta$  heterodimer have important roles in the nuclear import of IGFBP-2. As it is known that the nuclear import of IGFBP-3 is mediated mainly through importin- $\beta$  and not importin- $\alpha$ , the same antibodies were also used to block the nuclear import of IGFBP-3. As previously shown by Schedlich *et al.*,<sup>37</sup> blocking importin- $\beta$  led to inhibition of IGFBP-3 nuclear import, while blocking importin- $\alpha$  had no significant effect (see also Supplementary Figure S2). The differential effects of these antibodies on IGFBP-2 and IGFBP-3 nuclear transport support the specificity of these antibodies as blocking reagents, and indicate that nuclear import of IGFBP-2 and -3 do not follow the same mechanisms. Inclusion of normal IgG in the transport buffer confirmed that the inhibition of nuclear import of either IGFBP-2 or IGFBP-3 were specific blocking effects of the importin- $\alpha$  and - $\beta$  antibodies, respectively (see also Supplementary Figure S3).

IGFBP-2 possesses a putative cNLS in the linker domain

IGFBPs translocate into the nucleus via nuclear import mechanisms involving the presence of a functional NLS sequence.<sup>36,38</sup> Sequence alignments of the corresponding residues in IGFBP-2 to the NLS sequences in IGFBP-3, -5 and -6 reveals no similar NLS in IGFBP-2. However, when the IGFBP-2 amino-acid sequence was analyzed by the program PSORT II<sup>42</sup> (Table 1), one putative NLS sequence was instead identified in the linker region of human IGFBP-2 at <sup>179</sup>P-K-K-L-R-PP<sub>185</sub>. This sequence overlaps exactly with that of our previously described IGFBP-2 heparin-binding domain (HBD),<sup>54</sup> as shown in Figure 3a. A similar overlap between the HBD and the NLS sequence, although not in the linker region, has been reported for both IGFBP-3 and IGFBP-5.<sup>52,53,55,56</sup> The putative IGFBP-2 cNLS sequence contains a single cluster of basic amino-acid residues similar to other nuclear proteins (Table 1) possessing a classical monopartite NLS sequence (cNLS; X-K-K/R-X-K/R-X).<sup>52,53</sup> As shown in Figure 3b, sequence alignment of this putative IGFBP-2 NLS sequence shows a high degree of conservation across its orthologues. This implies the functional importance of the IGFBP-2 NLS sequence, and its consequent nuclear actions.

IGFBP-2 nuclear import is primarily mediated by importin- $\alpha$

To demonstrate the presence of potential IGFBP-2/importin- $\alpha$  or - $\beta$  interactions, a series of immunoprecipitation (IP) experiments were carried out using anti-IGFBP-2, importin- $\alpha$  and importin- $\beta$  on cell extracts from SHEP stable clones and SHEP cells over-expressing wild-type IGFBP-2 (SHEP-Wt-IGFBP-2). Specific bands for IGFBP-2 were detected only in whole cell extract from SHEP-Wt-IGFBP-2 cells and not SHEP cells (Figure 4a).

Following IP with anti-importin- $\alpha$  and - $\beta$  in SHEP-Wt-IGFBP-2, an immunoreactive band for IGFBP-2 was detected at 32 kDa only with anti-importin- $\alpha$  (Figure 4b; Supplementary Figure S4). The fact that importin- $\alpha$  was able to pull down IGFBP-2 suggests that importin- $\alpha$  may interact with IGFBP-2, potentially forming a complex. In contrast, no bands for IGFBP-2 were detected



**Table 1.** Alignment of predicted IGFBP-2 NLS vs well-established nuclear proteins containing a similar monopartite NLS sequence

NLS source <sup>a</sup>	Monopartite NLS sequence						M <sub>r</sub> (kDa)	Importin α/β	Reference
	P1	P2	P3	P4					
SV40 large T	K	K	K	R	K	V	90	α	(Kalderon <i>et al.</i> <sup>29</sup> )
Polyoma virus large T	R	K	R	P	R	P	98	α	(Richardson <i>et al.</i> <sup>43</sup> )
Human c-Myc	A	K	R	V	K	L	49	—	(Dang and Lee <sup>44</sup> )
c-jun and v-jun	S	R	K	R	K	L	65	β	(Chida and Vogt 1992 <sup>45</sup> ; Tagawa, Kuroki <i>et al.</i> 1995 <sup>46</sup> ; Forwood, Lam <i>et al.</i> <sup>47</sup> )
BRMS1	S	K	R	K	K	A	28	α	(Rivera <i>et al.</i> <sup>48</sup> )
Ku80	A	K	K	L	K	T	80	α	(Koike, Ikuta <i>et al.</i> 1999) <sup>49</sup>
FGF-1	Y	K	K	P	K	L		—	(Imamura, Engleka <i>et al.</i> 1990 <sup>50</sup> ; Imamura, Tokita <i>et al.</i> 1992) <sup>51</sup>
IGFBP-2	P	K	K	L	K	P	32		
Consensus sequence		K	K/R	x	K/R				(Chelsky <i>et al.</i> <sup>52</sup> ; Lange <i>et al.</i> <sup>53</sup> )

Abbreviations: BRMS1, breast cancer metastasis suppressor; c-Jun, cellular Jun; c-myc, oncogenic transcription factor; NLS, nuclear localization signal; v-Jun, viral version of Jun. <sup>a</sup>SV40 large T antigen is a hexamer protein that is a proto-oncogene; Polyoma virus large T antigen is a nuclear phosphoprotein that helps to regulate viral replication and gene expression; the Jun protein is a member of the AP-1 transcription factor family. BRMS1 is a member of a metastasis suppressor family; Ku80 is a subunit of Ku antigen complex (Ku70/Ku80) involved in DNA repair.

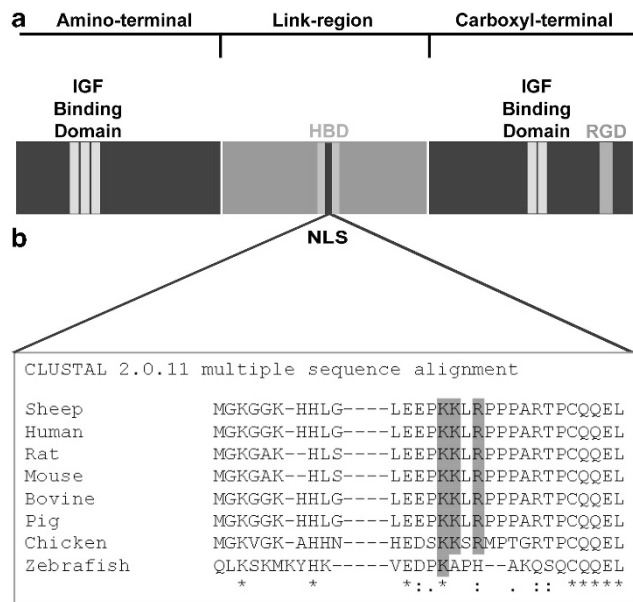


**Figure 3.** IGFBP-2 possesses a single putative NLS sequence that shows evolutionary conservation. **(a)** PSORT II analysis identified a classical monopartite NLS sequence in the linker domain of full-length IGFBP-2. **(b)** CLUSTAL multiple sequence alignment analysis shows high sequence conservation between human IGFBP-2 NLS and its orthologues. Residues shaded in gray indicate amino acids that are conserved.

in ‘bound’ material from IP with importin-β (Figure 4c; Supplementary Figure S4). These data are consistent with that shown by structural studies demonstrating that cNLS sequences are mainly recognized by the nuclear import receptor importin-α. These results are consistent with the above nuclear import assays, where we showed that IGFBP-2 nuclear uptake was significantly inhibited by immuno-depleting importin-α from the RRL system, while immuno-depletion of importin-β had no effect on nuclear import of IGFBP-2. No bands for IGFBP-2 were detected in any of the IPs performed on non-IGFBP-2-expressing SHEP cells.

We also carried out IP experiments on cell extracts from stable clones of SHEP cells overexpressing the NLS<sub>mut</sub>IGFBP-2 (SHEP-NLS<sub>mut</sub>IGFBP-2), to demonstrate the requirement of the IGFBP-2

NLS sequence for specific interaction with importin-α. In contrast to Wt-IGFBP-2, the NLS<sub>mut</sub>IGFBP-2 did not bind to importin-α as shown in Figure 4d. This was not surprising because the NLS sequence of IGFBP-2 was mutated by substituting two key amino acids previously shown to be crucial for ablation of NLS and importin-α interactions in other systems.<sup>57</sup>

IGFBP-2 contains an active/functional monopartite cNLS sequence To determine the contribution of the cNLS sequence to the nuclear import of the IGFBP-2 protein, we used the mutant NLS<sub>mut</sub>IGFBP-2, in which the key residues 179PKKL<sub>185</sub>, known to be critical in monopartite cNLS sequences, were mutated to 179PNNL<sub>185</sub>. As mentioned above, we had previously generated and completely characterized this mutant form of IGFBP-2 as HBD<sub>mut</sub>IGFBP-2.<sup>54</sup> We have thus utilized the HBD<sub>mut</sub>IGFBP-2, but renamed it NLS<sub>mut</sub>IGFBP-2, for consistency and relevance to these studies. As shown in Figure 5, the stable clones for SHEP-IGFBP-2 (wild type) and SHEP-NLS<sub>mut</sub>BP-2 were closely matched for IGFBP-2 mRNA expression (Figure 5b) and protein levels (Figure 5c). We have also shown that by introducing these mutations, the binding affinity of IGFBP-2 for IGF-I and IGF-II is not significantly altered.<sup>54</sup> IGF-binding affinity of the NLS<sub>mut</sub>IGFBP-2 (IGF-I K<sub>d</sub><sub>nm</sub> 1.45 ± 0.35; IGF-II K<sub>d</sub><sub>nm</sub> 0.52 ± 0.16) is similar to that of native IGFBP-2 (IGF-I K<sub>d</sub><sub>nm</sub> 1.14 ± 0.31; IGF-II K<sub>d</sub><sub>nm</sub> 0.37 ± 0.11). Western ligand blotting, (<sup>125</sup>I-IGF-I) of conditioned medium from Wt-IGFBP-2 or NLS<sub>mut</sub>IGFBP-2 SHEP cells, in Figure 5d, also showed similar band intensities. Furthermore, IGF-affinity chromatography was used to purify our native and mutant form of IGFBP-2 (Figure 5e). All the commercial anti-hIGFBP-2 used in these studies recognized the NLS<sub>mut</sub>IGFBP-2 and Wt-IGFBP-2 specifically and to the same degree (Figure 5f), as we have also shown previously.<sup>54</sup>

To determine the effect of the NLS mutation on IGFBP-2 nuclear localization, whole cell lysates from SHEP-pCMV (control), SHEP-IGFBP-2 and SHEP-NLS<sub>mut</sub>IGFBP-2 were subjected to cell fractionation (Figure 6a). A 32 kDa band for IGFBP-2 was present in the cytoplasmic fractions of SHEP-IGFBP-2 and SHEP-NLS<sub>mut</sub>BP-2 cell lines, while IGFBP-2 was only detected within the nuclear fraction of the SHEP-IGFBP-2 cells and not in the SHEP-NLS<sub>mut</sub>BP-2 cells (Figure 6a). Immunofluorescence for IGFBP-2 in these stable clones showed that IGFBP-2 was primarily present in the cytoplasm and only a small fraction detected intranuclear (Figure 6b). In contrast, NLS<sub>mut</sub>IGFBP-2 was only present in the cytoplasm and the perinucleus, and absent from the nucleus.

IGFBP-2 nuclear import is mediated by a cNLS and is a saturable process

To confirm at the cellular level the inability of NLS<sub>mut</sub>IGFBP-2 to translocate into the nucleus, we carried out nuclear import assays using affinity-purified NLS<sub>mut</sub>IGFBP-2 protein under the same conditions as for Wt-IGFBP-2 (Figure 2a). Wt-IGFBP-2 was imported into the nucleus (Figure 7a), while NLS<sub>mut</sub>IGFBP-2 accumulated in the perinucleus. These results were consistent with the cell fractionation and immunofluorescence studies of IGFBP-2 in SHEP-NLS<sub>mut</sub>BP-2 cells (Figure 6). To further investigate the requirement of the IGFBP-2 NLS sequence for its nuclear transport, IGFBP-2-derived peptides containing the wild-type NLS (W-NLS) (KHHLGLEEPKKLRPPPAR) or the mutated NLS sequence (NHHLGLEEPNNLAPPPAA) were employed to inhibit Wt-IGFBP-2

interaction with its nuclear transporter. IGFBP-2 nuclear entry was blunted in the presence of W-NLS peptide in 100-fold molar excess, but not by the same concentration of a mutated NLS peptide (Figure 7b). Collectively, these results demonstrate that the IGFBP-2 NLS sequence is required for targeting IGFBP-2 into the nucleus and that the IGFBP-2 nuclear import pathway, similar to that of other IGFBPs, is a saturable process.

#### NLS<sub>mut</sub>IGFBP-2 lacks the intranuclear functions of IGFBP-2

To determine whether the absence of nuclear IGFBP-2, as seen with the NLS<sub>mut</sub>IGFBP-2, has functional consequences, we investigated VEGF transcriptional regulation in our stable clones overexpressing Wt-IGFBP-2 or NLS<sub>mut</sub>IGFBP-2. VEGF mRNA was only upregulated in SHEP-Wt-IGFBP-2 and not in SHEP-NLS<sub>mut</sub>IGFBP-2 cells (Figure 8a), suggesting that intranuclear IGFBP-2 is required for activation of VEGF transcription. We further investigated this by transfection of a VEGF-promoter Luciferase construct<sup>23,55</sup> into SHEP cells stably overexpressing either Wt-IGFBP-2, NLS<sub>mut</sub>IGFBP-2 or the empty vector pCMV. Consistent with the mRNA data, the transcriptional activation of the VEGF promoter was enhanced only in SHEP-Wt-IGFBP-2 cells and not in SHEP-NLS<sub>mut</sub>IGFBP-2 (Figure 8b).

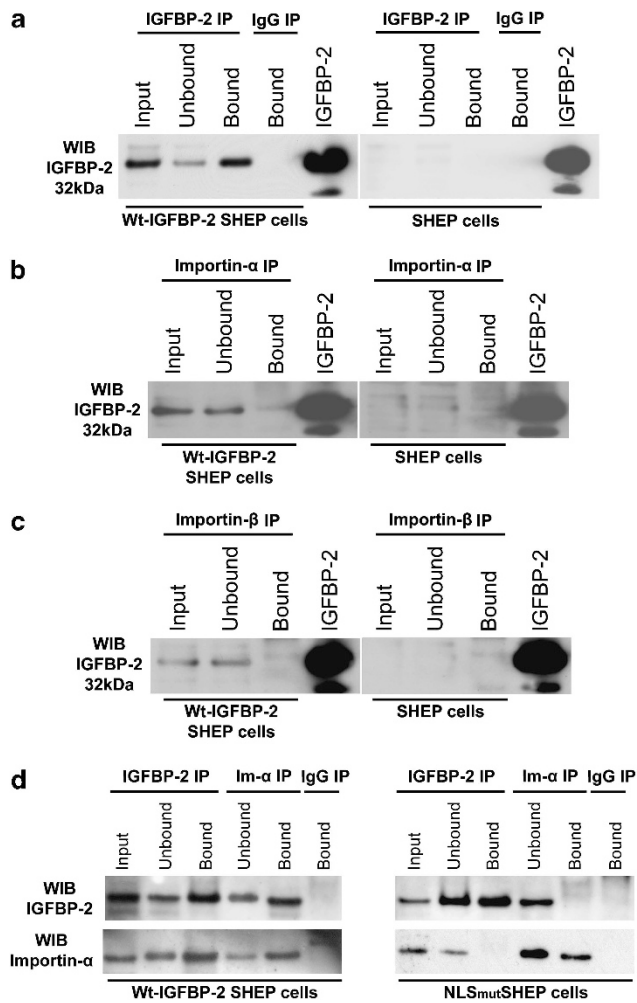


**Figure 4.** IGFBP-2 nuclear import is primarily mediated by importin- $\alpha$ . Immunoblotting with IGFBP-2 antibody detected a specific 32 kDa band in cell extracts from Wt-IGFBP-2 SHEP cells (SHEP cells overexpressing wild-type IGFBP-2) immunoprecipitated with anti-IGFBP-2 (a) and anti-importin- $\alpha$  (b), but not in cell extracts immunoprecipitated with anti-importin- $\beta$  (c) and in cell extracts from SHEP cells (not expressing IGFBP-2). (d) A specific 32 kDa band for IGFBP-2 was also detected in cell extracts from the SHEP cells overexpressing NLS<sub>mut</sub>-IGFBP-2 (see also Figure 5), but was not detected in these same cell extracts immunoprecipitated with anti-importin- $\alpha$ . No immunoreactive bands were detected with the IgG-negative control. Purified IGFBP-2 (10 ng) was also included as a control for anti-IGFBP-2 antibody specificity. Input, whole cell extract; unbound, post-IP material and bound, pull-down proteins/complexes by specific antibodies.

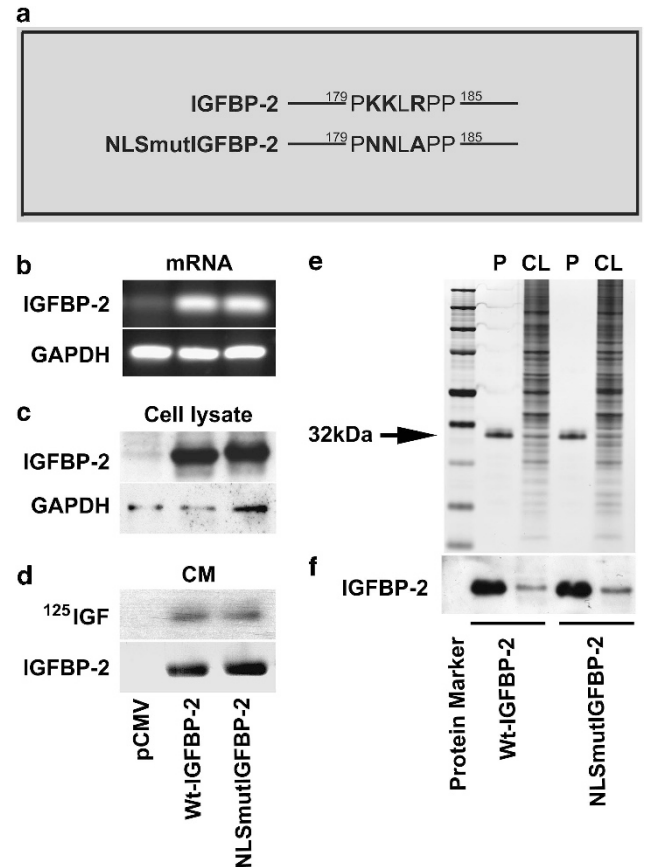


**Figure 5.** Mutagenesis of the IGFBP-2 putative NLS sequence. (a) The NLS sequence at 179PKKLRPP<sub>185</sub> was mutated to 179PNNLAPP<sub>185</sub> by PCR-based mutagenesis. (b and c) PCR and immunoblot showing IGFBP-2 expression levels in Wt-IGFBP-2 and NLS<sub>mut</sub>IGFBP-2 cells. (d) WLB showing <sup>125</sup>I-IGF binding for both forms of IGFBP-2 and immunoblot to confirm the presence of similar levels of IGFBP-2 in conditioned medium (CM). (e) Silver staining demonstrating presence of IGFBP-2 in cell lysate (CL) and quality of purified (P) recombinant Wt-IGFBP-2 or NLS<sub>mut</sub>IGFBP-2. (f) Immunoblot with anti-IGFBP-2 antibody for Wt-IGFBP-2 or NLS<sub>mut</sub>IGFBP-2 for confirmation of identity.

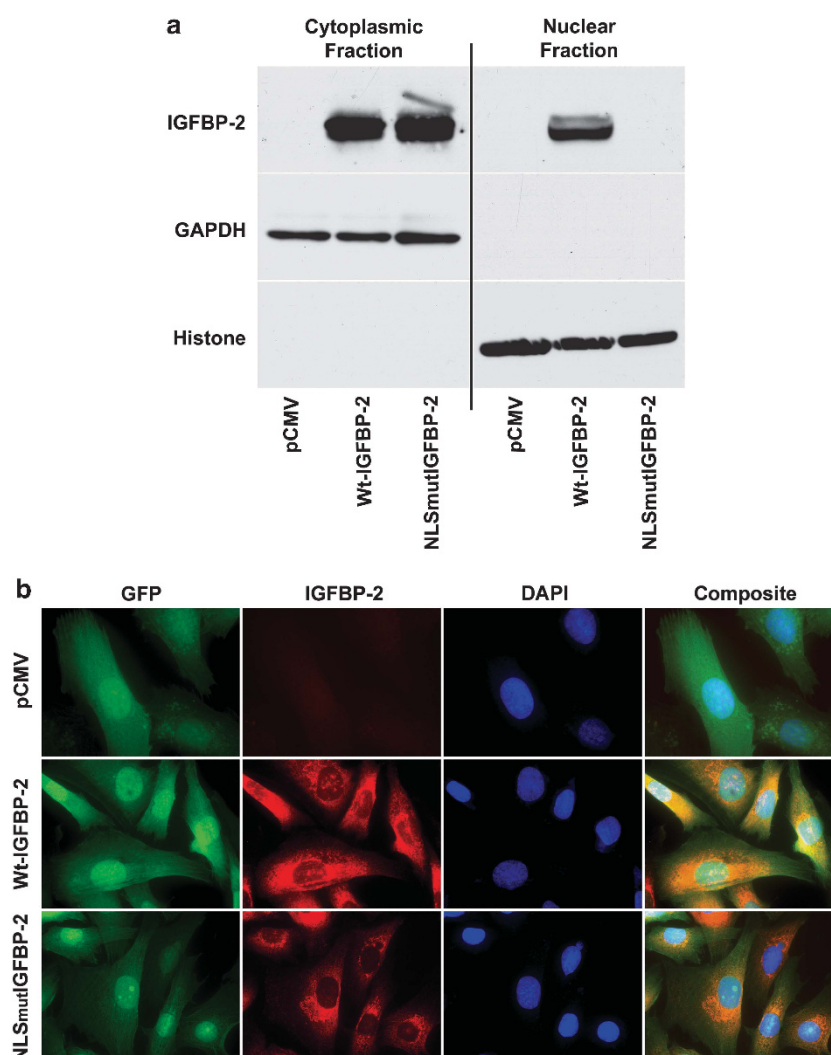


**Figure 6.** NLS<sub>mut</sub>IGFBP-2 does not translocate into the nucleus. **(a)** Cell fractionation of SHEP cells overexpressing Wt-IGFBP-2 or NLS<sub>mut</sub>IGFBP-2 demonstrated that Wt-IGFBP-2 is present in both the cytoplasmic and nuclear compartments, while NLS<sub>mut</sub>IGFBP-2 is only present in the cytoplasmic fraction. (Histone, nuclear marker; GAPDH, cytoplasmic marker). **(b)** IGFBP-2 immunofluorescence of pCMV-SHEP, Wt-IGFBP-2-SHEP and SHEP-NLS<sub>mut</sub>IGFBP-2 cells.

To demonstrate that upregulation of VEGF mRNA was mediated by intranuclear IGFBP-2, SHEP cells were transfected with the VEGF-promoter Luciferase construct in the presence or absence of Wt-IGFBP-2 or NLS<sub>mut</sub>IGFBP-2 protein, with or without the intracellular protein delivery reagent (TA) Chariot (Figure 8c). While VEGF promoter activity was enhanced in the presence of Wt-IGFBP-2 + TA (Figure 8c), no enhancement of the VEGF promoter was observed with NLS<sub>mut</sub>IGFBP-2 + TA. Consistent with these findings, no luciferase activity was observed in the absence of TA (that is, the protein remains in the extracellular/pericellular space) in both Wt-IGFBP-2 and NLS<sub>mut</sub>IGFBP-2, suggesting that the activation of the VEGF gene promoter is independent of any pericellular/cell-surface action of IGFBP-2, but requires intranuclear IGFBP-2. We also carried out a set of luciferase assays using VEGF promoter deletion constructs (Figure 8d) and confirmed that IGFBP-2-mediated activation of the VEGF promoter (VEGF-2.6) was lost with the VEGF-0.35 and VEGF-0.2 constructs, and partially reduced with the VEGF-1.5 construct. In contrast, none of the constructs showed NLS<sub>mut</sub>IGFBP-2 activation of luciferase activity, suggesting that nuclear IGFBP-2 is a key for transcriptional activation of VEGF.

#### NLS<sub>mut</sub>IGFBP-2 fails to induce angiogenesis *in vivo*

To assess whether overexpression of the NLS<sub>mut</sub>IGFBP-2 in SHEP cells elicits angiogenic activity *in vivo*, we employed the blood vessel network of the quail embryo chorio-allantoic membrane (CAM) assay, as previously described.<sup>23</sup> Consistent with our VEGF promoter luciferase assays and VEGF mRNA data, micro-neovascularization was clearly visible around and engulfing (red arrows in the enlargement of Figure 9) the implanted (black arrow) three-dimensional SHEP-WT-IGFBP-2 cell cultures. No angiogenesis was seen in the implanted three-dimensional SHEP-NLS<sub>mut</sub>IGFBP-2 cell cultures (enlargement of Figure 9) or in the control three-dimensional SHEP-pCMV cell implants. These findings provide further evidence for a role of nuclear IGFBP-2 in transcriptional activation of the VEGF gene and subsequently in angiogenesis.

#### DISCUSSION

Beyond its canonical IGF-dependent functions, IGFBP-2 exerts IGF-independent actions through interactions with the extracellular matrix, cell surface<sup>12,19,54,58</sup> or other putative receptors.<sup>1,56,59</sup> However, there is now increasing evidence to suggest that



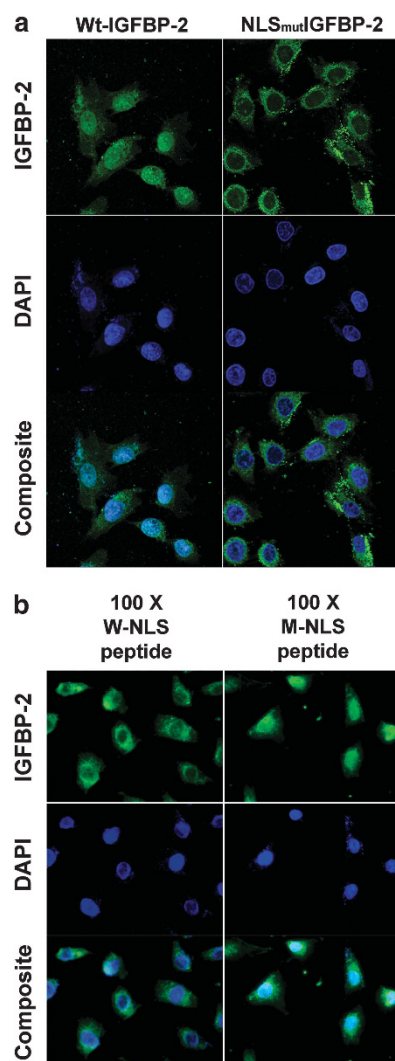


**Figure 7.** IGFBP-2 nuclear import is mediated by cNLS and is a saturable process. **(a)** Import assay showing IGFBP-2 nuclear import following permeabilization of the plasma membrane. SHEP cells were incubated in the presence of Wt-IGFBP-2 or NLS<sub>mut</sub>IGFBP-2 in transport buffer containing RRL and an ATP-regenerating system. **(b)** Competition experiments were carried out in digitonin-treated SHEP cells with transport buffer containing an ATP-regenerating system and RRL pre-incubated with peptide in 10 $\times$  or 100 $\times$  excess, either mimicking the Wt-IGFBP-2 NLS or NLS<sub>mut</sub>IGFBP-2 sequence. Data for 10 $\times$  of either peptide is not shown. Images are representative of at least three independent experiments. Cells were visualized by laser scanning confocal microscope (Leica TCS SP2 SE, objective  $\times$  63, oil immersion).

IGFBPs, including IGFBP-2, have intranuclear actions. Our studies demonstrate intranuclear localization of IGFBP-2, and for the first time, its mediation through a classical nuclear import pathway. We have identified and characterized a functional cNLS sequence in IGFBP-2 and shown that lack of nuclear translocation of IGFBP-2 prevents its pro-tumorigenic actions. We speculate that a novel mechanism of action for IGFBP-2 is via intranuclear actions, presumably via an IGF-independent pathway.

Our data confirm that IGFBP-2 localizes to the nucleus in common cancer cells, as suggested in previous studies.<sup>20–22,24</sup> The first report of intranuclear IGFBP-2 was in oxidant-exposed lung epithelial cells.<sup>22</sup> IGFBP-2 transgenic mice demonstrated perinuclear IGFBP-2 in several tissues,<sup>24</sup> while nuclear IGFBP-2

was seen in mouse lung epithelial cells (MLE-12), human prostate cancer (LnCap) cells<sup>20,21</sup> and human neuroblastoma (SK-N-SHEP).<sup>23</sup> However, the precise mechanism by which IGFBP-2 translocates into the nucleus remains elusive.

Proteins under 40–60 kDa can passively diffuse through nuclear pores; however, most proteins with nuclear functions use active carrier-mediated transport pathways. Although at 32 kDa, IGFBP-2 could theoretically enter the nucleus passively, by *in vitro* nuclear import assays we demonstrate that IGFBP-2 translocation into the nucleus is an active process, as shown for other proteins of a comparable molecular size.<sup>36,38,46,56,57,60–62</sup> Furthermore, NLS<sub>mut</sub>IGFBP-2, having an identical molecular size to that of wild-type IGFBP-2, did not enter the nucleus under any of the conditions examined, suggesting that the cNLS is necessary for its nuclear translocation. Similar to other IGFBPs, we have shown that a peptide spanning the NLS region prevented IGFBP-2 nuclear uptake, indicating that the mechanism involved is a specific and saturable process. Given recent insights into specific intranuclear actions of IGFBP-2, it is not surprising that IGFBP-2 nuclear import is mediated by an active and highly regulated pathway.

We also investigated the role of cytosolic receptor molecules, importin- $\alpha$  and - $\beta$ , in the nuclear import of IGFBP-2. The classical nuclear import pathway comprises the adaptor molecule importin- $\alpha$ , which mediates the interaction between the cargo molecule and the transport carrier importin- $\beta$ .<sup>63,64</sup> Importin- $\alpha$  recognizes cytosolic cargo by binding the cNLS sequence and shuttles through the nuclear pore in a complex with importin- $\beta$ . However, some cargo proteins bypass the requirement for an adaptor and bind directly to importin- $\beta$ .<sup>47,65,66</sup> Our nuclear import assays, with the inclusion of antibodies for importin- $\alpha$  and - $\beta$ , suggest that importin- $\alpha$  is more likely to mediate the nuclear uptake of IGFBP-2. This is consistent with other nuclear proteins containing similar monopartite cNLS sequences. Furthermore, our IP experiments suggest that importin- $\alpha$  recognizes the cNLS sequence of IGFBP-2, potentially mediating its nuclear uptake. This is in alignment with the fact that most proteins with a monopartite NLS sequence are recognized by importin- $\alpha$  and form a complex through the NLS-binding site. Our *in vitro* import data thus strongly indicate that importin- $\alpha$  mediates IGFBP-2 nuclear import. In order to definitively demonstrate this interaction, however, it would be necessary to complement our *in vitro* assay data with data showing that the direct interaction between IGFBP-2 and importin- $\alpha$  is disrupted upon addition of RanGTP.<sup>67</sup> Several members of the IGFBP family have been shown to translocate into the nucleus via the classical nuclear import pathway, using a bipartite nuclear localization sequence.<sup>36,38</sup> In contrast, IGFBP-2 possesses a monopartite NLS sequence within the basic motif located in the linker domain, a region mainly associated with binding to the cell surface/extracellular matrix,<sup>54,68</sup> and we have now shown that it is also required for the nuclear uptake of IGFBP-2. Interestingly, the NLS sequence of IGFBP-3 is also located in the basic motif known to be involved in binding to the cell surface/extracellular matrix<sup>36</sup> and other proteins,<sup>69–74</sup> thus reflecting the multifunctional significance of these domains across different IGFBPs. The conservation of this putative NLS sequence among IGFBP-2 orthologues suggests that this sequence has a critical role in IGFBP-2 nuclear translocation. We have tested this hypothesis by utilizing our previously described HBD<sub>mut</sub>IGFBP-2, which overlaps with the NLS sequence and provides us with a useful tool to examine IGFBP-2 nuclear import. Our findings are consistent with those reported by others, in which corresponding residues of the classical monopartite NLS sequence were similarly mutated, and consequently affected the nuclear activity of proteins, including SV40 Tag,<sup>36,75,76</sup> Polyomavirus large T,<sup>43</sup> c-myc,<sup>44</sup> Ku80<sup>44</sup> and FGF-1.<sup>77,78</sup>

Furthermore, we examined whether lack of intranuclear localization of IGFBP-2 had any functional consequences. Pro-tumorigenic actions of IGFBP-2 were completely abolished by

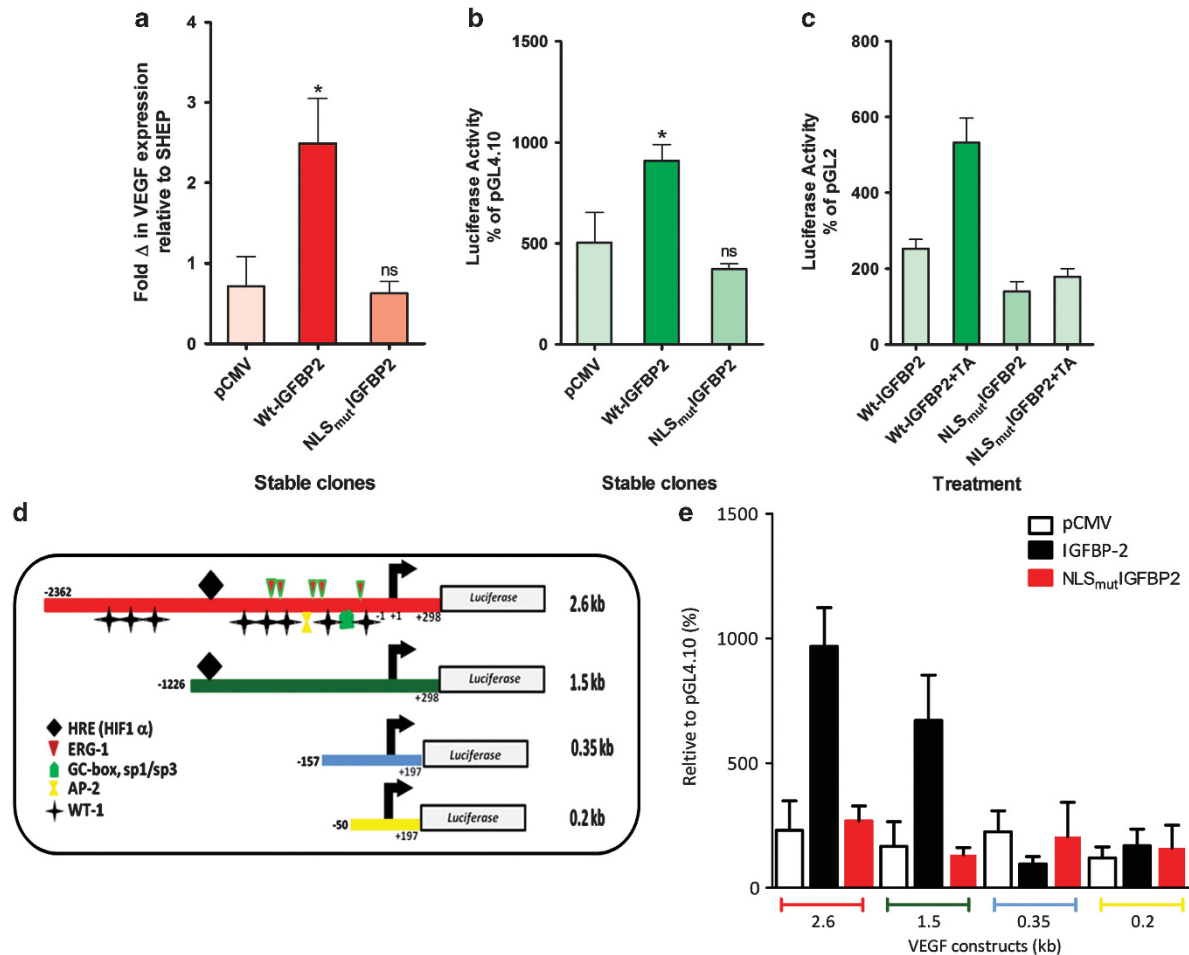


**Figure 8.** NLS<sub>mut</sub>IGFBP-2 lacks intranuclear functions of IGFBP-2. **(a)** RT-PCR showing VEGF mRNA expression levels in stable clones overexpressing Wt-IGFBP-2, NLS<sub>mut</sub>IGFBP-2 and empty vector control (pCMV). **(b)** Lack of transcriptional activation of the VEGF gene by the NLS<sub>mut</sub>IGFBP-2 clone was then verified via transfection of a VEGF-promoter luciferase construct into the same stable clones. **(c)** SHEP cells transfected with the VEGF-promoter luciferase construct in the presence or absence of Wt-IGFBP-2 or NLS<sub>mut</sub>IGFBP-2 protein  $\pm$  Chariot protein delivery reagent (TA). **(d)** Stable pCMV, Wt-IGFBP-2 and NLS<sub>mut</sub>IGFBP-2 cells transfected with deletion constructs of the VEGF promoter. **(e)** Error bars represent the means (s.d.) of three independent experiments, each run in duplicate.

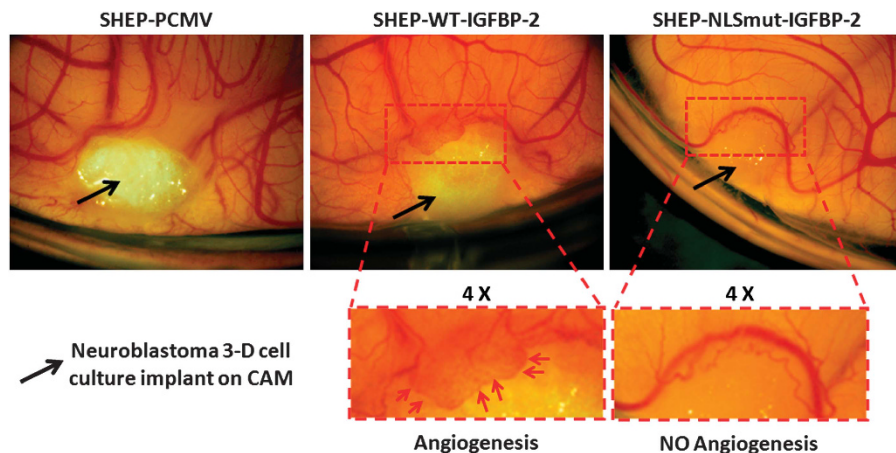


**Figure 9.** The NLS<sub>mut</sub>IGFBP-2 fails to induce angiogenesis *in vivo*. CAM assay showing potential angiogenic activity promoted by the neuroblastoma SHEP clones *in vivo*, as described in Materials and methods. Micro-neovascularization was monitored for up to 72 h (shown). After 72 h, micro-neovascularization was visible in a large area around and engulfing the implant of SHEP cells overexpressing IGFBP-2 (high VEGF expression), as shown in the enlarged section and indicated by the black arrows. Similar to the empty vector pCMV control, overexpression of NLS<sub>mut</sub>IGFBP-2 in SHEP cells did not result in activation of angiogenic processes, as shown in the enlarged section and indicated by the green arrows.



mutation of the NLS sequence, as evidenced in our NLS<sub>mut</sub>IGFBP-2. As we have recently demonstrated, nuclear IGFBP-2 is required for activation of angiogenic processes in neuroblastoma cells. In these studies, we demonstrate that VEGF expression was not enhanced in cells overexpressing NLS<sub>mut</sub>IGFBP-2, and we did not observe the occurrence of angiogenic processes. We also demonstrated that nuclear IGFBP-2 directly regulates VEGF expression, as suggested by the specific and selective activation of VEGF promoter deletion constructs by IGFBP-2. These data raise the possibility that IGFBP-2 could potentially act as a transcription factor. In order to definitively determine such a role for IGFBP-2, further experiments such as chromatin immunoprecipitation assays would be required.

In conclusion, we have shown that IGFBP-2 translocates into the nuclei of common cancer cells, an event mediated by a monopartite cNLS motif. In the nucleus, IGFBP-2 may bind directly to DNA and act as a transcription factor regulating the expression of tumorigenic genes, as we have recently reported.<sup>23</sup> Alternatively, the action of nuclear IGFBP-2 may be exerted indirectly through interactions with other nuclear proteins, and these events might potentially lead to intracellular/intranuclear modulation of processes, such as gene expression and cell cycle.

Whether nuclear IGFBP-2 derives from the secreted extracellular pool of IGFBP-2, which has re-entered the cell (autocrine), or derives from the intracellular pool of synthesized IGFBP-2 via an intracrine mechanism<sup>77,78</sup> is not clear and requires further investigation. Thus, despite current uncertainties regarding the origins of nuclear IGFBP-2, understanding the events that lead to its nuclear localization has provided insights into its role and the mechanisms behind its activation of processes involved in the promotion of tumorigenesis.

## MATERIALS AND METHODS

### Cell culture

The neuroblastoma SK-N-SHEP (SHEP) cell line and the stable clones SHEP-pCMV, SHEP-Wt-IGFBP-2 and SHEP-NLS<sub>mut</sub>IGFBP-2 (SHEP-HBD<sub>mut</sub>IGFBP-2) were obtained as previously described.<sup>54</sup> These cells were grown in 10% fetal calf serum/DMEM (Trace Biosciences, Castle Hill, NSW, Australia) or serum-free DMEM as indicated. Cells were cultured in the presence of neomycin (G-418 at 350 µg/ml, Gibco, Life Technologies Australia Pty Ltd, Mulgrave, VIC, Australia).<sup>23</sup>

### Prediction of IGFBP-2 NLS sequence and multiple sequence alignment

The IGFBP-2 amino-acid sequence was analyzed using the bioinformatics program PSORT II (<http://psort.nibb.ac.jp/form2.html>) to detect potential NLS sequences.<sup>42</sup> Multiple sequence alignment was carried out using ClustalX2 on the following accession sequences: *Mus musculus*, AAB60709; *Bs Taurus*, NP\_776980.1; *Sus scrofa*, NP\_999168.1; *Homo sapiens*, NP\_000588.2; *Ovis aries*, AAB23135.1; *Rattus norvegicus*, NP\_037254.2; *Gallus gallus*, NP\_990690.1 and *Danio rerio*, AAB56331.1.

### NLS<sub>mut</sub>IGFBP-2 mutagenesis and characterization

The mutagenesis strategy for the NLS domain of IGFBP-2 is identical to what we have previously described for the mutagenesis of the HBD sequence of IGFBP-2.<sup>54</sup> However, we have renamed HBD<sub>mut</sub>IGFBP-2 to NLS<sub>mut</sub>IGFBP-2 for relevance to these studies. WT or NLS<sub>mut</sub>IGFBP-2 in cell-conditioned medium was detected by western ligand blotting (WLB) using <sup>125</sup>I-IGF-I and immunoblotting. Native or NLS mutant IGFBP-2 was purified with IGF-I affinity chromatography and analyzed by silver staining, WLB (<sup>125</sup>I-IGF-I) and immunoblotting. Binding affinity for WT or NLS<sub>mut</sub>IGFBP-2 for either IGF-I or -II was determined as previously described.<sup>54</sup>

### Nuclear transport assay

Nuclear transport assays with purified IGFBP-2 or NLS<sub>mut</sub>IGFBP-2 protein were carried out on SHEP cells as previously described.<sup>23</sup> Transport assays were also carried out in the presence of anti-importin-α or -β (PA1-5811 and MA3-070; Thermo Scientific, Scoresby, VIC, Australia) and in the presence or absence of rabbit-reticulocyte-lysate (RRL), respectively, to

examine their roles in IGFBP-2 nuclear import. To further demonstrate the specificity of the NLS sequence for IGFBP-2 interaction with importins, peptides containing the WT NLS (W-NLS; KHLGLLEEPKKLRPPPAR) or the mutated NLS sequence (NLS-mut; NHHGLLEEPNNLAPPPAA) (Mimotopes Pty. Ltd., Melbourne, VIC, Australia) were used at concentrations of 10-fold and 100-fold molar excess of full-length IGFBP-2, to compete with IGFBP-2 interaction with importins. Transport assays were stopped by washing with cold phosphate-buffered saline and the subcellular localization of IGFBP-2 was determined using immunofluorescence, as previously described,<sup>79</sup> using the following antibodies: anti-IGFBP-2 and IGFBP-3 (1:200; Santa Cruz Biotechnology Inc., Santa Cruz, CA, USA), anti-goat Fluoro 488 (1:500; Molecular Probes, Bleiswijk, Netherlands) or Alexa Fluor 568 phalloidin (1:500; Life Technologies Australia Pty Ltd, Melbourne, VIC, Australia) followed by 4',6-diamidino-2-phenylindole (1:5000; Chemicon, Temecula, CA, USA) staining for 20 min. Omission of the primary antibody or mouse IgG formed the negative controls. Nuclear transport assays for IGFBP-3 (ref. 36) were also carried out simultaneously under the various conditions, forming the positive controls. Microscopy was performed on a Leica TCS SP2 SE Laser Scanning Confocal Microscope with dual- and triple-channel detection optics (Leica Microsystems, North Ryde, NSW, Australia). To acquire an image of the emission from each fluorophore, the sections were analyzed with appropriate filters using single or simultaneous excitation at 488 nm (fluorescein isothiocyanate), 594 nm (Texas red) or 405 nm (4',6-diamidino-2-phenylindole). Images were collected under identical non-saturated conditions after multiple scans, averaging 10–12 sections per cell. Sections were sequentially scanned to ensure that any observed co-expression was not owing to overlap of excitation, nor emission spectra of fluorophores. Images were collected and analyzed using Leica LCS Lite software.

### Cell fractionation, SDS-PAGE, Immunoblotting and IP

For isolation of cytoplasmic and nuclear fractions, cells were treated and immunoblotting performed ( $n = 3$ ) as previously described.<sup>23</sup>

**Immunoprecipitation.** Following cell pellet extraction from SHEP-Wt-IGFBP-2, SHEP-NLS<sub>mut</sub>IGFBP-2 and SHEP cells with IP buffer (Tris 100 mM, ethylenediaminetetraacetic acid 5 mM, NaCl 150 mM, 0.1% bovine serum albumin with 1% sodium deoxycholate, 1% Triton X-100 and protease inhibitors), 80 µl of prewashed 25% protein G-Sepharose suspension was added to each sample and incubated for 2 h at 4 °C, followed by centrifugation at 5000 r.p.m. for 10 min at 4 °C. The supernatant was transferred to fresh tubes and anti-IGFBP-2 (SC-6001, C-18) or anti-importin-α/β were added to a final dilution of 1:100, after addition of 100 µl of fresh 25% protein G-Sepharose suspension, and incubated overnight at 4 °C with gentle agitation. Samples were centrifuged as above and washed three times with cold IP buffer before separation with 3–15% SDS-PAGE, followed by immunoblotting with anti-IGFBP-2. Purified IGFBP-2 and IgG IP were included as positive and negative controls, respectively.

### IGFBP-2 protein transfection

SHEP cells ( $0.3 \times 10^6$ ) were seeded in 6-well tissue culture plates with DMEM containing 10% fetal calf serum. When cells reached 40–50% confluency, the media were aspirated and cells washed once with phosphate-buffered saline. Purified IGFBP-2 or NLS<sub>mut</sub>IGFBP-2 (500 ng) was resuspended in sterile Dulbecco-phosphate-buffered saline (100 µl) and mixed 1:1 with the diluted (1/16) Chariot reagent (Active Motif, Carlsbad, CA, USA) before addition to the cell monolayer. Cells were incubated in serum-free medium at 37 °C in a humidified atmosphere containing 5% CO<sub>2</sub> for 24 h, as per the manufacturer's specifications.

### VEGF-promoter luciferase constructs and reporter assays

The luciferase reporter plasmids driven by a 2326 bp human VEGF promoter construct<sup>55</sup> or the 1.5 kb, 0.35 kb and 0.2 kb deletion constructs<sup>55</sup> and a *Renilla* Luciferase control vector (pRL-TK; Promega, Alexandria, NSW, Australia) were used in this study as previously described.<sup>23</sup>

### In vivo angiogenesis—quail embryo CAM assay

This was essentially performed as we previously described.<sup>23</sup>

## Total RNA extraction, RT-PCR and quantitative PCR

Cells were grown as above and total RNA extracted and processed using the RNeasy Minikit (Qiagen, Valencia, CA, USA) and the RNase-free DNase kit (Ambion, Austin, TX, USA).

**RT-PCR.** All reverse transcription and PCR reactions were performed using the GeneAmp PCR Core kit (Applied Biosystems, Life Technologies Australia Pty Ltd, Mulgrave, VIC, Australia) as previously described. Gene-specific primers that were analyzed include GAPDH 5'-CCATGGCACCCT-CAAGGCTGA-3', 5'-GGCCATCCACAGTCTTCTGG-3' and VEGF 5'-AGGAG-GAGGGCAGAATCATCA-3', 5'-ctcgattggatggcagtagct-3' (Sigma Chemical Co., St Louis, MO, USA).

## Statistical analysis

RT-PCR experiments were performed three times on complementary DNA from three independent experiments. Luciferase assays were performed three times and readings were normalized to the empty vector pGL4.10. Data were analyzed by GraphPad (La Jolla, CA, USA) PRISM-5 software using t-test and/or one-way analysis of variance, with the data presented as mean  $\pm$  s.e.m. or s.d. of three independent experiments.

## CONFLICT OF INTEREST

The authors declare no conflict of interest.

## ACKNOWLEDGEMENTS

We wish to thank Professor Dev Mukhopadhyay (Mayo Clinic, Rochester, MN, USA) for kindly supplying the VEGF constructs used in these studies, Dr Mark Denham (Neuroscience, University of Melbourne) for his assistance in developing the GFP-SHEP cells clones, Dr Donald Newgreen (MCRI) for his assistance in developing CAM assays and Dr Sheena Azar for constant assistance during manuscript preparation. This work was supported by the National Health and Medical Research Council (NHMRC) of Australia Project Grants 1008062 (to GAW and VCR). WJA is the recipient of a Melbourne University (MRS) PhD scholarship.

## REFERENCES

- Firth SM, Baxter RC. Cellular actions of the insulin-like growth factor binding proteins. *Endocr Rev* 2002; **23**: 824–854.
- Jones JL, Clemmons DR. Insulin-like growth factors and their binding proteins: biological actions. *Endocr Rev* 1995; **16**: 3–34.
- Cohen P, Peehl DM, Stamey TA, Wilson KF, Clemmons DR, Rosenfeld RG. Elevated levels of insulin-like growth factor-binding protein-2 in the serum of prostate cancer patients. *J Clin Endocrinol Metab* 1993; **76**: 1031–1035.
- Busund LT, Richardsen E, Busund R, Ukkonen T, Bjornsen T, Busch C *et al*. Significant expression of igfbp2 in breast cancer compared with benign lesions. *J Clin Pathol* 2005; **58**: 361–366.
- So AI, Levitt RJ, Eigl B, Fazli L, Muramaki M, Leung S *et al*. Insulin-like growth factor binding protein-2 is a novel therapeutic target associated with breast cancer. *Clin Cancer Res* 2008; **14**: 6944–6954.
- Fuller GN, Rhee CH, Hess KR, Caskey LS, Wang R, Bruner JM *et al*. Reactivation of insulin-like growth factor binding protein 2 expression in glioblastoma multiforme: a revelation by parallel gene expression profiling. *Cancer Res* 1999; **59**: 4228–4232.
- Song SW, Fuller GN, Khan A, Kong S, Shen W, Taylor E *et al*. IGF-1R, an insulin-like growth factor binding protein 2 (igfbp-2) binding protein, antagonizes igfbp-2 stimulation of glioma cell invasion. *Proc Natl Acad Sci USA* 2003; **100**: 13970–13975.
- Wang H, Shen W, Huang H, Hu L, Ramdas L, Zhou YH *et al*. Insulin-like growth factor binding protein 2 enhances glioblastoma invasion by activating invasion-enhancing genes. *Cancer Res* 2003; **63**: 4315–4321.
- Elmlinger MW, Deininger MH, Schuett BS, Meyermann R, Duffner F, Grote EH *et al*. In vivo expression of insulin-like growth factor-binding protein-2 in human gliomas increases with the tumor grade. *Endocrinology* 2001; **142**: 1652–1658.
- Moore MG, Wetterau LA, Francis MJ, Peehl DM, Cohen P. Novel stimulatory role for insulin-like growth factor binding protein-2 in prostate cancer cells. *Int J Cancer* 2003; **105**: 14–19.
- Flyvbjerg A, Mogensen O, Mogensen B, Nielsen OS. Elevated serum insulin-like growth factor-binding protein 2 (igfbp-2) and decreased igfbp-3 in epithelial ovarian cancer: correlation with cancer antigen 125 and tumor-associated trypsin inhibitor. *J Clin Endocrinol Metab* 1997; **82**: 2308–2313.

- Pereira JJ, Meyer T, Docherty SE, Reid HH, Marshall J, Thompson EW *et al*. Bimolecular interaction of insulin-like growth factor (igf) binding protein-2 with alphavbeta3 negatively modulates igf-I-mediated migration and tumor growth. *Cancer Res* 2004; **64**: 977–984.
- Fukushima T, Tezuka T, Shimomura T, Nakano S, Kataoka H. Silencing of insulin-like growth factor-binding protein-2 in human glioblastoma cells reduces both invasiveness and expression of progression-associated gene cd24. *J Biol Chem* 2007; **282**: 18634–18644.
- Oh Y, Yamanaka Y, Kim HS, Vorwerk P, Wilson E, Hwa V *et al*. IGF-independent actions of igfbps. In: Takano K, Hizuka N, Takahashi SI (eds) *Molecular Mechanisms to Regulate the Activities of Insulin-like Growth Factors*. Elsevier Science Bv: Amsterdam, 1998, pp 125–133.
- Mohan S, Baylink DJ. IGF-binding proteins are multifunctional and act via igf-dependent and -independent mechanisms. *J Endocrinol* 2002; **175**: 19–31.
- Russo VC, Bach LA, Fosang AJ, Baker NL, Werther GA. Insulin-like growth factor binding protein-2 binds to cell surface proteoglycans in the rat brain olfactory bulb. *Endocrinology* 1997; **138**: 4858–4867.
- Russo VC, Schutt BS, Andaloro E, Ymer SI, Hoeflich A, Fosang A *et al*. Igfbp-2/igf-1/Proteoglycan Complexes in the Rat Brain Olfactory Bulb. *12th International Congress of Endocrinology Medimont International Proceedings* 2004, ISBN 88-7587-071-3(CD ISBN 88-7587-072-1 817–820.
- Perks CM, Newcomb PV, Norman MR, Holly JM. Effect of insulin-like growth factor binding protein-1 on integrin signalling and the induction of apoptosis in human breast cancer cells. *J Mol Endocrinol* 1999; **22**: 141–150.
- Schutt B, Langkamp M, Rauschnabel U, Ranke M, Elmlinger M. Integrin-mediated action of insulin-like growth factor binding protein-2 in tumor cells. *J Mol Endocrinol* 2004; **32**: 859–868.
- Terrien X, Bonvin E, Corroyer S, Tabary O, Clement A, Henrion Caude A. Intracellular colocalization and interaction of igf-binding protein-2 with the cyclin-dependent kinase inhibitor p21cip1/waf1 during growth inhibition. *Biochem J* 2005; **392**: 457–465.
- Miyako K, Cobb LJ, Francis M, Huang A, Peng B, Pintar JE *et al*. Papa-1 is a nuclear binding partner of igfbp-2 and modulates its growth-promoting actions. *Mol Endocrinol* 2009; **23**: 169–175.
- Besnard V, Corroyer S, Trugnan G, Chadelat K, Nabeyrat E, Cazals V *et al*. Distinct patterns of insulin-like growth factor binding protein (igfbp)-2 and igfbp-3 expression in oxidant exposed lung epithelial cells. *Biochim Biophys Acta* 2001; **1538**: 47–58.
- Azar WJ, Azar SHX, Higgins S, Hu JF, Hoffman AR, Newgreen DF *et al*. Igfbp-2 enhances vegf gene promoter activity and consequent promotion of angiogenesis by neuroblastoma cells. *Endocrinology* 2011; **152**: 3332–3342.
- Hoeflich A, Reisinger R, Schuett BS, Elmlinger MW, Russo VC, Vargas GA *et al*. Peri/nuclear localization of intact insulin-like growth factor binding protein-2 and a distinct carboxyl-terminal igfbp-2 fragment in vivo. *Biochem Biophys Res Commun* 2004; **324**: 705–710.
- Gorlich D, Mattaj JW. Protein kinesin—nucleocytoplasmic transport. *Science* 1996; **271**: 1513–1518.
- Mattaj JW, Englmeier L. Nucleocytoplasmic transport: the soluble phase. *Annu Rev Biochem* 1998; **67**: 265–306.
- Dingwall C, Laskey RA. Nuclear targeting sequences—a consensus. *Trends Biochem Sci* 1991; **16**: 478–481.
- Kalderon D, Roberts BL, Richardson WD, Smith AE. A short amino-acid sequence able to specify nuclear location. *Cell* 1984; **39**: 499–509.
- Kalderon D, Richardson WD, Markham AF, Smith AE. Sequence requirements for nuclear location of simian virus-40 large-t-antigen. *Nature* 1984; **311**: 33–38.
- Robbins J, Dilworth SM, Laskey RA, Dingwall C. 2 interdependent basic domains in nucleoplasmic nuclear targeting sequence—identification of a class of bipartite nuclear targeting sequence. *Cell* 1991; **64**: 615–623.
- Chook YM, Blobel G. Karyopherins and nuclear import. *Curr Opin Struct Biol* 2001; **11**: 703–715.
- Cingolani G, Bednenko J, Gillespie MT, Gerace L. Molecular basis for the recognition of a nonclassical nuclear localization signal by importin beta. *Mol Cell* 2002; **10**: 1345–1353.
- Catimel B, Teh T, Fontes MRM, Jennings IG, Jans DA, Howlett GJ *et al*. Biophysical characterization of interactions involving importin-alpha during nuclear import. *J Biol Chem* 2001; **276**: 34189–34198.
- Schedlich LJ, O'Han MK, Leong GM, Baxter RC. Insulin-like growth factor binding protein-3 prevents retinoid receptor heterodimerization: implications for retinoic acid-sensitivity in human breast cancer cells. *Biochem Biophys Res Commun* 2004; **314**: 83–88.
- Schedlich LJ, Muthukaruppan A, O'Han MK, Baxter RC. Insulin-like growth factor binding protein-5 interacts with the vitamin d receptor and modulates the vitamin d response in osteoblasts. *Mol Endocrinol* 2007; **21**: 2378–2390.

- 36 Schedlich LJ, Young TF, Firth SM, Baxter RC. Insulin-like growth factor-binding protein (igfbp)-3 and igfbp-5 share a common nuclear transport pathway in t47d human breast carcinoma cells. *J Biol Chem* 1998; **273**: 18347–18352.
- 37 Schedlich LJ, Le Page SL, Firth SM, Briggs LJ, Jans DA, Baxter RC. Nuclear import of insulin-like growth factor-binding protein-3 and -5 is mediated by the importin beta subunit [in process citation]. *J Biol Chem* 2000; **275**: 23462–23470.
- 38 Iosef C, Gkourasas T, Jia CYH, Li SS-C, Han VKM. A functional nuclear localization signal in insulin-like growth factor binding protein-6 mediates its nuclear import. *Endocrinology* 2008; **149**: 1214–1226.
- 39 Chi NC, Adam EJH, Adam SA. Sequence and characterization of cytoplasmic nuclear-protein import factor p97. *J Cell Biol* 1995; **130**: 265–274.
- 40 Kehlenbach RH, Dickmanns A, Gerace L. Nucleocytoplasmic shuttling factors including ran and crm1 mediate nuclear export of nfat *in vitro*. *J Cell Biol* 1998; **141**: 863–874.
- 41 Ivanova IA, Vespa A, Dagnino L. A novel mechanism of e2f1 regulation via nucleocytoplasmic shuttling—determinants of nuclear import and export. *Cell Cycle* 2007; **6**: 2186–2195.
- 42 Nakai K, Horton P. Psort: a program for detecting sorting signals in proteins and predicting their subcellular localization. *Trends Biochem Sci* 1999; **24**: 34–35.
- 43 Richardson WD, Roberts BL, Smith AE. Nuclear location signals in polyoma-virus large-t. *Cell* 1986; **44**: 77–85.
- 44 Dang CV, Lee WMF. Identification of the human c-myc protein nuclear translocation signal. *Mol Cell Biol* 1988; **8**: 4048–4054.
- 45 Chida K, Vogt PK. Nuclear translocation of viral Jun but not of cellular Jun is cell cycle dependent. *PNAS* 1992; **89**: 4290–4292.
- 46 Tagawa T, Kuroki T, Vogt PK, Chida K. The cell cycle-dependent nuclear import of v-Jun is regulated by phosphorylation of a serine adjacent to the nuclear-localization signal. *J Cell Biol* 1995; **130**: 255–263.
- 47 Forwood JK, Lam MHC, Jans DA. Nuclear import of creb and ap-1 transcription factors requires importin-beta 1 and ran but is independent of importin-alpha. *Biochemistry* 2001; **40**: 5208–5217.
- 48 Rivera J, Megias D, Navas C, Bravo J. Identification of essential sequences for cellular localization in brms1 metastasis suppressor. *Plos One* 2009; **4**: e4633.
- 49 Koike M, Ikuta T, Miyasaka T, Shiomi T. Ku80 can translocate to the nucleus independent of the translocation of Ku70 using its own nuclear localization signal. *Oncogene* 1999; **18**: 7495–7505.
- 50 Imamura T, Engleka K, Zhan X, Tokita Y, Forough R, Roeder D et al. Recovery of mitogenic activity of a growth factor mutant with a nuclear translocation sequence. *Science* 1990; **249**: 1567–1570.
- 51 Imamura T, Tokita Y, Mitsui Y. Identification of a heparin-binding growth factor-1 nuclear translocation sequence by deletion mutation analysis. *J Biol Chem* 1992; **267**: 5676–5679.
- 52 Chelsky D, Ralph R, Jonak G. Sequence requirements for synthetic peptide-mediated translocation to the nucleus. *Mol Cell Biol* 1989; **9**: 2487–2492.
- 53 Lange A, Mills RE, Lange CJ, Stewart M, Devine SE, Corbett AH. Classical nuclear localization signals: definition, function, and interaction with importin alpha. *J Biol Chem* 2007; **282**: 5101–5105.
- 54 Russo VC, Schutt BS, Andaloro E, Ymer SI, Hoeflich A, Ranke MB et al. Insulin-like growth factor binding protein-2 binding to extracellular matrix plays a critical role in neuroblastoma cell proliferation, migration, and invasion. *Endocrinology* 2005; **146**: 4445–4455.
- 55 Mukhopadhyay D, Knebelmann B, Cohen HT, Ananth S, Sukhatme VP. The von hippel-lindau tumor suppressor gene product interacts with sp1 to repress vascular endothelial growth factor promoter activity. *Mol Cell Biol* 1997; **17**: 5629–5639.
- 56 Ben-Shmuel A, Shvab A, Gavert N, Brabletz T, Ben-Ze'ev A. Global analysis of l1-transcriptomes identified igfbp-2as a target of ezrin and nf-kappab signaling that promotes colon cancer progression. *Oncogene* 2012; **6**: 340.
- 57 Marfori M, Lonhienne TG, Forwood JK, Kobe B. Structural basis of high-affinity nuclear localization signal interactions with importin-a. *Traffic* 2012; **13**: 532–548.
- 58 Russo VC, Bach LA, Werther GA. Cell membrane association of insulin-like growth factor binding protein-2 (igfbp-2) in the rat brain olfactory bulb. *Prog Growth Factor Res* 1995; **6**: 329–336.
- 59 Shen X, Xi G, Maile LA, Wai C, Rosen CJ, Clemmons DR. Insulin-like growth factor binding protein-2 functions coordinately with receptor protein tyrosine phosphatase beta and the igf-i receptor to regulate igf-i-stimulated signaling. *Mol Cell Biol* 2012; **32**: 4116–4130.
- 60 Zhou GL, Doci CL, Lingen MW. Identification and functional analysis of nol7 nuclear and nucleolar localization signals. *BMC Cell Biol* 2010; **11**: 74.
- 61 Lufei CC, Cao XM. Nuclear import of pin1 is mediated by a novel sequence in the ppiase domain. *FEBS Lett* 2009; **583**: 271–276.
- 62 Breeuwer M, Goldfarb DS. Facilitated nuclear transport of histone h1 and other small nucleophilic proteins. *Cell* 1990; **60**: 999–1008.
- 63 Gorlich D, Prehn S, Laskey RA, Hartmann E. Isolation of a protein that is essential for the first step of nuclear-protein import. *Cell* 1994; **79**: 767–778.
- 64 Adam EJH, Adam SA. Identification of cytosolic factors required for nuclear location sequence-mediated binding to the nuclear-envelope. *J Cell Biol* 1994; **125**: 547–555.
- 65 Forwood JK, Harley V, Jans DA. The c-terminal nuclear localization signal of the sex determining region y (sry) high mobility group domain mediates nuclear import through beta 1. *J Biol Chem* 2001; **276**: 46575–46582.
- 66 Forwood JK, Harley V, Jans DA. The c-terminal nuclear localisation signal of the sry hmg domain mediates nuclear import through importin beta. *Mol Biol Cell* 2001; **12**: 500A-A.
- 67 Lee SJ, Matsuura Y, Liu SM, Stewart M. Structural basis for nuclear import complex dissociation by rangtp. *Nature* 2005; **435**: 693–696.
- 68 Russo VC, Gluckman P, Feldman EL, Werther GA. The insulin-like growth factor system and its pleiotropic functions in brain. *Endocr Rev* 2005; **26**: 916–943.
- 69 Firth SM, Ganeshprasad U, Baxter RC. Structural determinants of ligand and cell surface binding of insulin-like growth factor-binding protein-3. *J Biol Chem* 1998; **273**: 2631–2638.
- 70 Twigg SM, Baxter RC. Insulin-like growth factor (igf)-binding protein 5 forms an alternative ternary complex with igfs and the acid-labile subunit. *J Biol Chem* 1998; **273**: 6074–6079.
- 71 Firth SM, Clemmons DR, Baxter RC. Mutagenesis of basic amino acids in the carboxyl-terminal region of insulin-like growth factor binding protein-5 affects acid-labile subunit binding. *Endocrinology* 2001; **142**: 2147.
- 72 Weinzimer SA, Gibson TB, Collett-Solberg PF, Khare A, Liu B, Cohen P. Transferrin is an insulin-like growth factor-binding protein-3 binding protein. *J Clin Endocrinol Metab* 2001; **86**: 1806–1813.
- 73 Nam TJ, Busby Jr. W, Clemmons DR. Insulin-like growth factor binding protein-5 binds to plasminogen activator inhibitor-i. *Endocrinology* 1997; **138**: 2972–2978.
- 74 Booth BA, Boes M, Andress DL, Dake BL, Kiefer MC, Maack C et al. Igfbp-3 and igfbp-5 association with endothelial cells: role of c-terminal heparin binding domain. *Growth Regul* 1995; **5**: 1–17.
- 75 Hodel MR, Corbett AH, Hodel AE. Dissection of a nuclear localization signal. *J Biol Chem* 2001; **276**: 1317–1325.
- 76 Hodel AE, Harreman MT, Pulliam KF, Harben ME, Holmes JS, Hodel MR et al. Nuclear localization signal receptor affinity correlates with *in vivo* localization in *saccharomyces cerevisiae*. *J Biol Chem* 2006; **281**: 23545–23556.
- 77 Dubois V, Couissi D, Schonne E, Schneider YJ, Remacle C, Trouet A. Estrogen and insulin modulation of intracellular insulin-like growth factor binding proteins in human breast cancer cells: possible involvement in lysosomal hydrolases over-secretion. *Biochem Biophys Res Commun* 1993; **192**: 295–301.
- 78 Butt AJ, Dickson KA, McDougall F, Baxter RC. Insulin-like growth factor-binding protein-5 inhibits the growth of human breast cancer cells *in vitro* and *in vivo*. *J Biol Chem* 2003; **278**: 29676–29685.
- 79 Higgins S, Wong SHX, Richner M, Rowe CL, Newgreen DF, Werther GA et al. Fibroblast growth factor 2 reactivates g1 checkpoint in sk-n-mc cells via regulation of p21, inhibitor of differentiation genes (id1-3), and epithelium-mesenchyme transition-like events. *Endocrinology* 2009; **150**: 4044–4055.

Supplementary Information accompanies this paper on the Oncogene website (<http://www.nature.com/onc>)